

Evaluation of genetically expressed absorbing proteins using photoacoustic spectroscopy

Jan Laufer^{a‡}, Amit Jathoul^{a†}, Martin Pule^{†+}, Paul Beard^{*+}

Department of Medical Physics & Bioengineering (*), the Centre for Advanced Biomedical Imaging, (+) and the UCL Cancer Institute (†), University College London, Gower Street, London WC1E 6BT
Julius Wolff Institut, Charité – Universitätsmedizin Berlin, Augustenburger Platz 1, 13353 Berlin, Germany (‡)

ABSTRACT

Genetically expressed contrast agents are of great interest in the life sciences as they allow the study of structure and function of living cells and organisms. However, many commonly used fluorescent proteins present disadvantages when used in mammalian organisms, such as low near-infrared absorption and photostability. In this study, a variety of genetically expressed fluorescent proteins and novel chromoproteins were evaluated using photoacoustic spectroscopy. The results showed that chromoproteins provide stronger photoacoustic signals, better spectral stability, and exhibit less photobleaching than fluorescent proteins.

Keywords: Photoacoustic spectroscopy, fluorescent proteins, chromoproteins, genetic expression

1. INTRODUCTION

Fluorescent proteins are widely used as reporter genes in preclinical research to study biological events, such as gene expression and apoptosis. In photoacoustic imaging¹, genetically expressed fluorescent proteins have been used in zebrafish and *Drosophila* (fruitfly) pupa by generating photoacoustic signals at excitation wavelengths that lie in the absorption band of the fluorophore. Although some genetically expressed fluorescent proteins exhibit absorption into the red wavelength region², relatively few provide strong absorption at near-infrared wavelengths where penetration depth in mammalian tissues is greatest. A rare example of a near-infrared fluorescent protein is iRFP³, a bacteriophytochrome-based protein with maximum absorption at 680nm, which has recently been used as a genetically expressed contrast agent for photoacoustic tumour imaging in mice⁴. As a consequence the potential use of most fluorescent proteins in mammalian small animal models is restricted to superficial imaging applications. In addition, many fluorescent proteins lack photostability, which can manifest itself as dark states⁵, blinking⁶, transient absorption⁷, and photobleaching⁸. Furthermore, little is known about their response to the high peak power laser pulses used in photoacoustic imaging - apart from the reduction in the amount of energy that is available for thermalisation, and hence the photoacoustic effect, due fluorescent emissions. Lastly, genetically expressed non-fluorescent proteins, called chromoproteins⁹, may be a suitable alternative for photoacoustic imaging. In this study, the efficiency with which photoacoustic signals are generated in fluorescent proteins and chromoproteins is evaluated using photoacoustic spectroscopy.

2. METHODS

2.1 Bacterial expression of fluorescent proteins and chromoproteins

The genes encoding the fluorescent proteins mCherry¹⁰, mNeptune¹¹, mRaspberry¹², and E2 Crimson¹³ and the chromoproteins aeCP597¹⁴ and cjBlue were synthesised in multiple stages. A gene encoding for a fluorescent protein or chromoprotein is assembled using commercially available oligonucleotide fragments¹⁵. The gene not only encodes the

^a Joint first authors.

protein of interest but also a glutathione-S-transferase (GST)-tag, which is later used for protein purification. The gene is introduced into bacteria (*Escherichia Coli* DH5 α , New England Biolabs, USA) by heat shock where the bacterial expression vector facilitates the protein expression. The fusion proteins were purified using resin according to manufacturer's instructions (Pierce Biotechnology Inc., USA). This provided samples of purified proteins dissolved in distilled water (50 – 100 μ l volume) for further characterisation using photoacoustic spectroscopy. Absorption spectra of these samples were measured using spectrophotometers (Varioskan Flash or NanoDrop, Thermo Scientific, USA).

2.2 Experimental set up

Samples of the purified fluorescent proteins and chromoproteins were characterised using the experimental set-up shown in Figure 1. A wavelength tuneable OPO laser system (Newport Spectra Physics / GWU GmbH) provided excitation pulses of 7 ns duration between 450 nm and 680 nm at a pulse repetition frequency of 50Hz. The output of the OPO laser illuminated a sample holder with a fluence of 1.2 mJ cm^{-2} to 1.7 mJ cm^{-2} depending on the excitation wavelength. The sample holder contained a volume of approximately 24 μ l and was placed in a shallow water bath to allow the propagation of photoacoustic waves, generated by the absorption of excitation laser pulses, to a Fabry-Pérot polymer film ultrasound sensor for detection. The photoacoustic signals were recorded using a digitising oscilloscope (Tektronix TDS5430) and downloaded to a PC. A portion was directed to an integrating sphere with an in-built wavelength-calibrated photodiode which was used to obtain a measure of the incident pulse energy in order to normalise the photoacoustic signals.

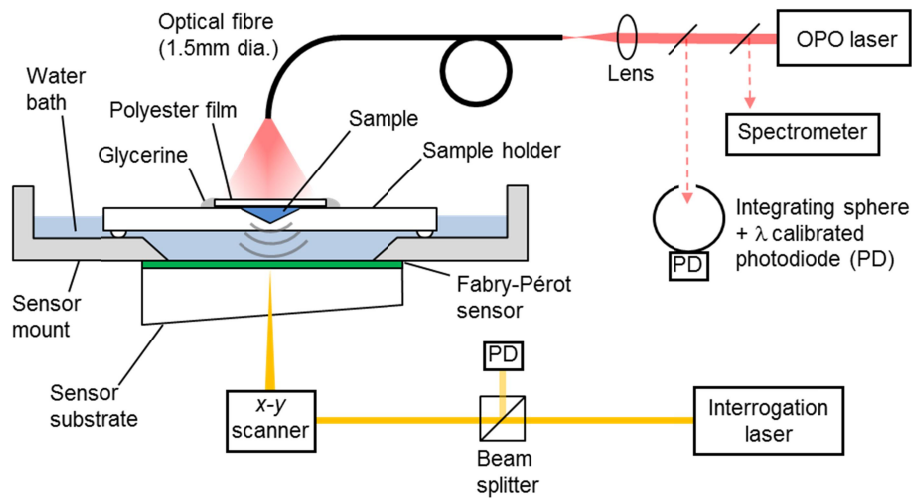


Figure 1 Experimental setup

To obtain the photoacoustic amplitude spectrum of a protein, the peak-to-peak values of photoacoustic signals generated at excitation wavelengths between 450 nm and 680 nm were recorded in 10nm steps. The protein concentrations of the solutions ranged from 20 to 80 μ M. Photoacoustic amplitude spectra were also measured in phosphate-buffered saline suspensions of both the normal type (NT) cells and human tumour cells (K562) expressing aeCP597. The shape of the photoacoustic spectra was then compared to those of purified proteins measured using optical transmission spectroscopy. Photobleaching was assessed by plotting the photoacoustic signal amplitude as a function of the number of laser pulses. The excitation wavelength was chosen to coincide with the absorption peak of a specific protein sample. The incident fluence was around 1.7 mJ cm^{-2} .

3. RESULTS

3.1 Photoacoustic amplitude spectra of fluorescent proteins

Figure 2 shows the photoacoustic amplitude spectra (circles) measured purified fluorescent proteins and their corresponding specific extinction spectra (dashed line), i.e. mCherry (Figure 2a), mRaspberry (Figure 2b), E2 Crimson

(Figure 2c), and mNeptune (Figure 2d). To allow a qualitative comparison of the shape of the amplitude spectrum with that of the specific extinction coefficient spectrum, the vertical scales of each graph were adjusted by eye until a reasonable match between the two types of spectra was achieved.

Significant differences between the shapes of the specific extinction spectra and the corresponding photoacoustic amplitude spectra were observed for all fluorescent proteins. The differences are most noticeable at wavelengths where the specific extinction coefficient is greatest and resulted in a double-peaked photoacoustic amplitude spectrum.

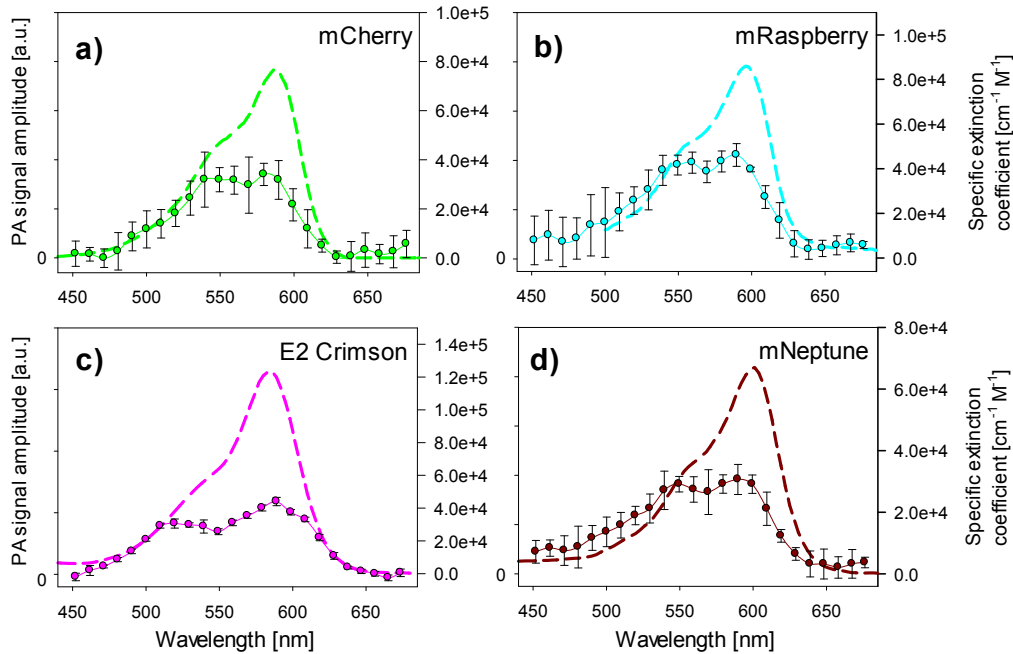


Figure 2 Photoacoustic spectra (circles) of purified fluorescent protein solutions of (a) mCherry, (b) mRaspberry, (c) E2 Crimson, (d) mNeptune together with their specific extinction coefficient spectra (dashed lines). The error bars represent the standard deviation of the measurements.

3.2 Photoacoustic amplitude spectra of chromoproteins

Figure 3 shows the photoacoustic amplitude spectra (circles) of the chromoproteins cjBlue and aeCP597, and their corresponding specific extinction spectra (dashed lines). The shape of the photoacoustic amplitude spectra are generally in good qualitative agreement with the specific extinction spectra and do not exhibit a double peak as seen in fluorescent proteins. In addition, their optical absorption extends further into the near-infrared wavelength region. For example, cjBlue exhibits significant absorption at wavelengths up to 650nm.

3.3 Photoacoustic amplitude spectra normalised to the absorption coefficient

The amplitude spectra were divided by the peak absorption coefficient of the sample solutions as measured by the spectrophotometer. Absorption normalisation allowed a direct comparison of the photoacoustic amplitude spectra of all proteins. This provided an indication of the efficiency with which photoacoustic signals are generated in each protein species, i.e. how much of the optical energy is thermalized and converted to pressure. Figure 4 shows photoacoustic amplitude spectra (represented as data points connected by a spline curve for better visualisation) of the chromoproteins aeCP597 and cjBlue, and the fluorescent proteins E2 Crimson, mNeptune, mRaspberry, and mCherry. The photoacoustic signal amplitude produced in the fluorescent proteins is less than half that observed in the chromoproteins, suggesting inefficient photoacoustic signal generation. Figure 4 clearly demonstrates that chromoproteins provide stronger photoacoustic signals than fluorescent proteins.

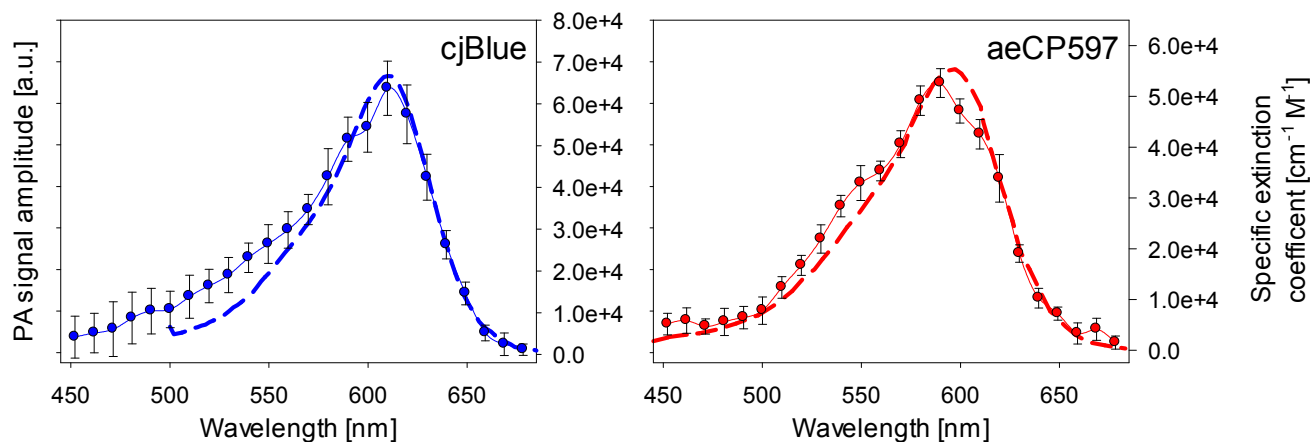


Figure 3 Photoacoustic spectra (circles) of purified chromoprotein solutions of cjBlue and aeCP597. The corresponding specific extinction coefficient spectra are shown as a dashed line. The error bars represent the standard deviation of the measurements.

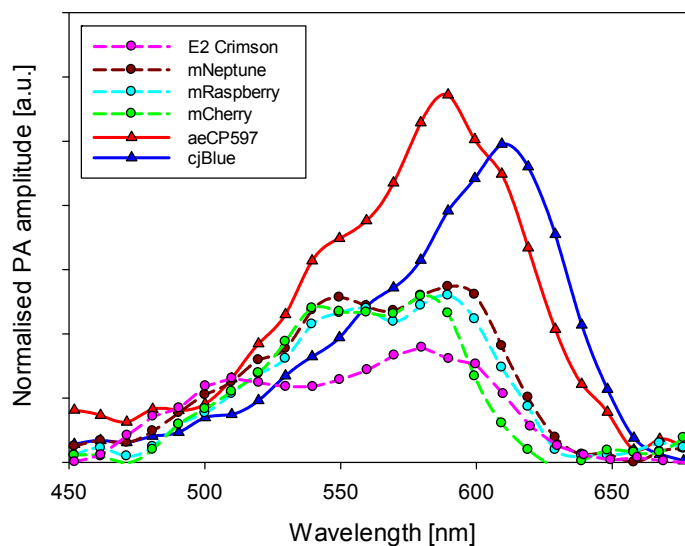


Figure 4 Absorption-normalised photoacoustic spectra of fluorescent proteins (mNeptune, mRaspberry, mCherry, E2 Crimson) and chromoproteins (aeCP597, cjBlue).

3.4 Photobleaching

To assess photobleaching, the protein samples were irradiated with laser pulses and the photoacoustic signal amplitude was recorded over time. To improve the visualisation of the results, a hyperbolic function was then fitted to the photobleaching curve and the determined coefficients were in turn used as input parameters to plot the decay curves. Figure 5 shows the change in the signal amplitude as a function of the number laser pulses for the fluorescent proteins and chromoproteins investigated in this study. Most fluorescent proteins exhibited a decrease in signal amplitude with increasing number of laser pulses. E2 Crimson was the exception and provided almost constant signal amplitude during the measurement. This is somewhat surprising since E2 Crimson has been shown to exhibit biphasic photobleaching in confocal microscopy¹³. By comparison, the average radiant power used to obtain the results shown in Figure 5 was orders of magnitude lower, which may explain the absence of photobleaching. In contrast to the majority of fluorescent proteins, the chromoproteins showed only minor photobleaching.

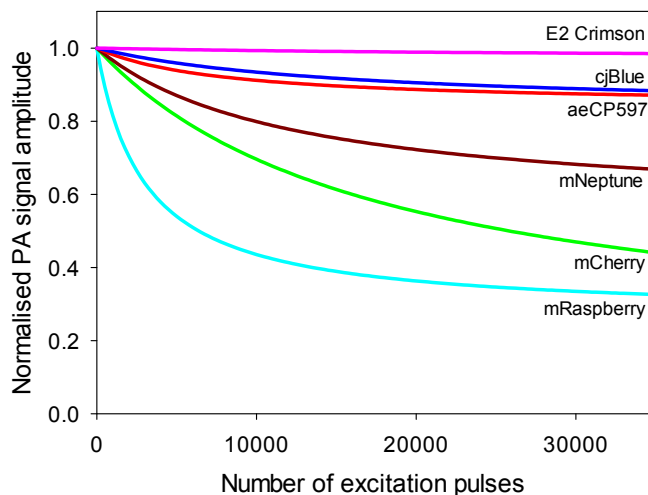


Figure 5 Photobleaching of fluorescent proteins and chromoproteins under prolonged exposure to nanosecond laser pulses. The fluence at the sample ranged from 1.5 to 1.7 mJ cm^{-2} .

4. DISCUSSION AND CONCLUSIONS

This study has shown that the photoacoustic signal amplitude generated in the fluorescent proteins is lower compared to the chromoproteins (Figure 4). In addition, the shapes of the photoacoustic amplitude spectra of the fluorescent proteins evaluated in this study are different to those of the corresponding extinction coefficient spectra (Figure 2) while good agreement was observed in chromoproteins (Figure 3). Lastly, fluorescent proteins show stronger photobleaching compared to chromoproteins (Figure 5).

The lower photoacoustic signal amplitudes in fluorescent proteins can be explained in part by the loss of energy due to fluorescent emissions. However, the absorption-normalised spectra suggest that additional mechanisms contribute to a reduced thermalisation of the optical excitation pulse. For example, ground state bleaching¹⁷ due to long electronic relaxation times is a likely cause. It occurs when a fraction of fluorescent molecules is promoted to an excited state, leaving less (or no) molecules available to facilitate ground state absorption. Since the electronic transitions involved in fluorescence and phosphorescence occur on sub-nanosecond to millisecond time scales¹⁸, early arriving photons of a nanosecond excitation pulse would encounter fluorescent proteins in the ground state while later arriving photons would also encounter proteins in the excited state. This reduces the nominal absorption coefficient at the excitation wavelength, and therefore the photoacoustic signal amplitude. Given that the electronic relaxation times (or fluorescence lifetimes) of many fluorescent proteins, including those investigated in this study, are of the order of nanoseconds¹⁹⁻²¹, ground state bleaching is therefore a likely cause of the reduced photoacoustic signal amplitude observed in this study. Chromoproteins, by contrast, do not fluoresce or phosphoresce and are likely to exhibit short, vibrational relaxations (of the order of ps). This would prevent ground state bleaching during ns excitation pulses and ensure efficient thermalisation and photoacoustic signal generation.

Another consequence of the long relaxation times seen in fluorescent proteins is irreversible photobleaching²². Long relaxation times increase the likelihood of electronic transitions via the triplet state, which can create highly reactive singlet oxygen that can damage the fluorophores, thus causing photobleaching²². Chromoproteins, owing to their fast relaxation times, are much less likely to generate singlet oxygen. This explanation agrees with the results of this study, which show that fluorescent proteins tend to photobleach much faster than chromoproteins.

While fluorescent energy loss and ground state bleaching may explain why fluorescent proteins produce lower photoacoustic signal amplitudes than chromoproteins, it is less straightforward to explain the difference in shape between the photoacoustic and corresponding optical absorption spectra. A possible reason may be the re-absorption and thermalisation of a portion of the fluorescent emission from one molecule by another (excited) molecule due to transient absorption. The total absorbed energy would then also depend upon the wavelength dependence of fluorescence, transient absorption, and ground state absorption. The combination of partial ground state absorption, ground state bleaching, and fluorescence absorption may explain the shapes of the photoacoustic spectra observed in this study.

The results of this study suggest that fluorescent proteins are less suitable for photoacoustic imaging than chromoproteins. However, while the chromoproteins evaluated in this work provided greater photoacoustic signal amplitude and exhibited lower photobleaching, it is unclear whether they are biocompatible and efficiently expressed in mammalian cells. Further development, similar to that many fluorescent proteins have undergone, may therefore be needed to establish chromoproteins as genetically expressed photoacoustic contrast agents.

REFERENCES

1. Beard, P. Biomedical photoacoustic imaging. *Interface focus* **1**, 602–631 (2011).
2. Shaner, N. C. *et al.* Improving the photostability of bright monomeric orange and red fluorescent proteins. *Nature Methods* **5**, 545–51 (2008).
3. Filonov, G. S. *et al.* Bright and stable near-infrared fluorescent protein for in vivo imaging. *Nature biotechnology* **29**, 757–61 (2011).
4. Filonov, G. S. *et al.* Deep-Tissue Photoacoustic Tomography of a Genetically Encoded Near-Infrared Fluorescent Probe. *Angewandte Chemie* **124**, 1477–1480 (2012).
5. Hendrix, J., Flors, C., Dedecker, P., Hofkens, J. & Engelborghs, Y. Dark states in monomeric red fluorescent proteins studied by fluorescence correlation and single molecule spectroscopy. *Biophysical Journal* **94**, 4103–4113 (2008).
6. Blum, C. & Subramaniam, V. Single-molecule spectroscopy of fluorescent proteins. *Analytical and bioanalytical chemistry* **393**, 527–41 (2009).
7. Stoner-Ma, D. *et al.* Observation of excited-state proton transfer in green fluorescent protein using ultrafast vibrational spectroscopy. *Journal of the American Chemical Society* **127**, 2864–5 (2005).
8. Strack, R. L. *et al.* A rapidly maturing far-red derivative of DsRed-Express2 for whole-cell labeling. *Biochemistry* **48**, 8279–81 (2009).
9. Shkrob, M. a *et al.* Far-red fluorescent proteins evolved from a blue chromoprotein from *Actinia equina*. *The Biochemical journal* **392**, 649–54 (2005).
10. Shaner, N. C. *et al.* Improved monomeric red, orange and yellow fluorescent proteins derived from *Discosoma* sp. red fluorescent protein. *Nature biotechnology* **22**, 1567–72 (2004).
11. Lin, M. Z. *et al.* Autofluorescent proteins with excitation in the optical window for intravital imaging in mammals. *Chemistry & Biology* **16**, 1169–79 (2009).
12. Wang, L., Jackson, W. C., Steinbach, P. a & Tsien, R. Y. Evolution of new nonantibody proteins via iterative somatic hypermutation. *Proc. of the Nat. Acad. of Sciences of the United States of America* **101**, 16745–9 (2004).
13. Strack, R. L. *et al.* A rapidly maturing far-red derivative of DsRed-Express2 for whole-cell labeling. *Biochemistry* **48**, 8279–81 (2009).
14. Shkrob, M. a *et al.* Far-red fluorescent proteins evolved from a blue chromoprotein from *Actinia equina*. *The Biochemical Journal* **392**, 649–54 (2005).
15. Stemmer, W. P., Cramer, a, Ha, K. D., Brennan, T. M. & Heyneker, H. L. Single-step assembly of a gene and entire plasmid from large numbers of oligodeoxyribonucleotides. *Gene* **164**, 49–53 (1995).
16. Warrens, A. N., Jones, M. D. & Lechler, R. I. Splicing by overlap extension by PCR using asymmetric amplification: an improved technique for the generation of hybrid proteins of immunological interest. *Gene* **186**, 29–35 (1997).
17. Ruckebusch, C., Sliwa, M., Pernot, P., De Juan, a. & Tauler, R. Comprehensive data analysis of femtosecond transient absorption spectra: A review. *Journal of Photochemistry and Photobiology C: Photochemistry Reviews* **13**, 1–27 (2012).
18. Borst, J. W. & Visser, A. J. W. G. Fluorescence lifetime imaging microscopy in life sciences. *Measurement Science and Technology* **21**, 102002 (2010).
19. Hendrix, J., Flors, C., Dedecker, P., Hofkens, J. & Y Dark states in monomeric red fluorescent proteins studied by fluorescence correlation and single molecule spectroscopy. *Biophysical journal* **94**, (2008).
20. Blum, C. & Subramaniam, V. Single-molecule spectroscopy of fluorescent proteins. *Analytical and bioanalytical chemistry* **393**, 527–41 (2009).
21. Cotlet, M. *et al.* Identification of different emitting species in the red fluorescent protein DsRed by means of ensemble and single-molecule spectroscopy. *Proceedings of the National Academy of Sciences of the United States of America* **98**, 14398–403 (2001).
22. Lichtman, J. W. & Conchello, J. Fluorescence microscopy. *Nature Methods* **2**, 910–9 (2005).